International Journal of Biological Macromolecules 239 (2023) 124286

Contents lists available at ScienceDirect

International Journal of Biological Macromolecules

journal homepage: www.elsevier.com/locate/ijbiomac

Interplay of electrolyte concentration and molecular weight of polyDADMAC on cellulose surface adsorption

Carina Sampl [a,b], Jana Schaubeder [a], Ulrich Hirn [a,b,*], Stefan Spirk [a,b]

[a] Institute of Bioproducts and Paper Technology, Graz University of Technology, Inffeldgasse 23, 8010 Graz, Austria
[b] Christian Doppler Laboratory for Fiber Swelling and Paper Performance, Graz University of Technology, Inffeldgasse 23, 8010 Graz, Austria

ARTICLE INFO

Keywords:
Regenerated cellulose model films
Trimethylsilyl cellulose
Cellulose xanthate
Polyelectrolyte, surface plasmon resonance
Quartz crystal microbalance with dissipation

ABSTRACT

Cationic polyelectrolytes (PEs) are commonly used additives in manufacturing of cellulose based products such as regenerated fibers and paper to tailor their product properties. Here we are studying the adsorption of poly (diallyldimethylammonium chloride), PD, on cellulose, using in situ surface plasmon resonance spectroscopy (SPR) measurements. We employ model surfaces from regenerated cellulose xanthate (CX) and trimethylsilyl cellulose (TMSC), mimicking industrially relevant regenerated cellulose substrates. The effects of the PDs molecular weight were strongly depending on the ionic strength and type of electrolyte (NaCl vs $CaCl_2$). Without electrolytes, the adsorption was monolayer-type, i.e. independent of molecular weight. At moderate ionic strength, adsorption increased due to more pronounced PE coiling, while at high ionic strength electrostatic shielding strongly reduced adsorption of PDs. Results exhibited pronounced differences for the chosen substrates (cellulose regenerated from xanthate (CX_{reg}) vs. regenerated from trimethylsilyl cellulose, $TMSC_{reg}$). Consistently higher adsorbed amounts of the PD were determined on CX_{reg} surfaces compared TMSC. This can be attributed to a more negative zeta potential, a higher AFM roughness and a higher degree of swelling (investigated by QCM-D) of the CX_{reg} substrates.

1. Introduction

Modification of cellulose fibers is a commonly employed procedure to realize tailor-made products in a variety of applications such as paper, textiles, medical materials and hygiene products, and others. In many cases, modification does not involve chemical formation of bonds but merely relies on the physical deposition of materials onto the fiber surfaces. Among these, polyelectrolytes (PEs) are frequently used modifiers that induce either positive or negative charge density on cellulose fibers.

The main driving force for the interaction and adsorption of PEs onto surfaces in general is electrostatic attraction which is further modulated by the adsorption conditions (e.g., pH value, PE concentration, ionic strength, temperature) and the surface properties (e.g., charge density, morphology, hydrophilicity) [1,2]. In the absence of electrolytes, PEs exhibit strong intra— and intermolecular electrostatic repulsion between their charged monomeric units, resulting in an elongated shape leading to a fairly inflexible conformation in aqueous solutions (Fig. 1b). In aqueous systems of higher ionic strength, however, the intra- and intermolecular electrostatic repulsion decreases due to screening of the charges by oppositely charged ions. This results in a more coiled, necklace-like structure (Fig. 1c) so that the polymer supports a more loosely bound conformation allowing for structural rearrangements [3–5]. Cationic PEs play an important role in paper production processes, where they are used as retention aids (e.g., cationic starch, PEI, PAA), strengthening agents (e.g., cationic starch) and fixation agents (PDADMAC) to finally obtain papers with desired properties.

Cationization of regenerated fibers in turn imparts antimicrobial activity (e.g., by chitosan), enabling a wide range of applications in medical and hygiene products that additionally feature tunable water uptake which is important in wound healing [6–13]. Cationization further facilitates the dyeability of regenerated fibers as many textile dyes carry anionic charge that are capable to form ion complexes with cationic PEs, thereby improving economic and ecologic performance of the dyeing process [14–17]. Consequently, there have been many studies aiming at optimizing the interaction conditions of fibers with a variety or PEs [18–25].

On industrially relevant regenerated cellulose fibers, the adsorption of different cationic PEs is mainly focusing on chitosan and its derivatives due to their antimicrobial action [26–28]. Only a limited

* Corresponding author at: Institute of Bioproducts and Paper Technology, Graz University of Technology, Inffeldgasse 23, 8010 Graz, Austria.
E-mail address: ulrich.hirn@tugraz.at (U. Hirn).

https://doi.org/10.1016/j.ijbiomac.2023.124286
Received 19 September 2022; Received in revised form 13 March 2023; Accepted 28 March 2023
Available online 1 April 2023

amount of publications is available studying the interaction of regenerated fibers with other PE types such as cationic starch, xylans, and other cellulose derivatives as monitoring of fiber adsorption processes is not trivial due to the complexity of the starting material [29–31]. Therefore, many studies aiming at elaboration of fundamentals of cellulose–PE interactions have been performed on cellulose thin films. These provide a defined morphology and chemistry, and enable the use of surface sensitive techniques to obtain real-time data. For instance, the adsorption of cationic cellulose/starch [32–35], chitosan [34,36], cationic polyacrylamide (C-PAM) [37–39] and poly(diallyldimethylammonium chloride, PD) [32,40–42] have been studied on these films. PD is a particularly relevant PE as it is frequently used in paper and fiber production to aid the removal of undesired substances from the water circulation systems, for modification of the fiber surface or to promote the retention of anionic dyes on cellulose surfaces [43]. PD is a highly charged cationic PE, which exhibits a permanently positively charged quaternary ammonium group per monomer unit (Fig. 1a) that can undergo strong interaction with oppositely charged materials in aqueous media.

In contrast to the few available works on PD adsorption on cellulose thin films that focused on multilayer formation [32,41,42], the present work aims at evaluating the effect of the molecular weight of PD and the impact of ionic strength on the adsorption onto regenerated cellulose thin films with different charge densities. The use of 2-D substrates, i.e. cellulose model thin films, excludes complex interactions due to the fibrous matrix in regenerated fibers and allows, in principle, to study the involved adsorption mechanisms and kinetics in real-time using surface plasmon resonance spectroscopy (SPR) and quartz-crystal microbalance with dissipation (QCM-D).

2. Experimental

2.1. Materials

Trimethylsilyl cellulose (TMSC, prepared from Avicel cellulose, DS_{Si} = 2.74 M_W = 181,000 g·mol^{-1}, M_n = 30,400 g·mol^{-1} PDI = 6.1 determined by SEC in chloroform) was purchased from TITK (Rudolstadt, Germany). Cellulose xanthate (CX) stock solution was provided by Kelheim Fibers (Kelheim, Germany) and used without further treatment. The CX stock solution was diluted with MQ water to obtain the desired concentration of 1.3 wt% and vigorously mixed using a vortex shaker for 30 s and afterwards filtered using a Chromafil Xtra PVDF-45/25 filter with 0.45 μm pore size diameter. For all experiments, MQ water (resistivity = 18 MΩ·cm) from a Millipore water purification system (Millipore, USA) was used. Chloroform (99.3 %), hydrogen peroxide (30 % in water), hydrochloric acid (37 %), diiodomethane (99 %) and sulfuric acid (95 %) were acquired from Sigma Aldrich and used as received.

PD samples from Sigma Aldrich applied in this study were used as received, i.e. a sample of low molecular weight PD (low) with M_w <100,000 g·mol^{-1}, medium molecular weight PD (med) M_w = 200,000–350,000 g·mol^{-1} and high molecular weight PD (high) of M_w > 400,000–500,000 g·mol^{-1}.

The industrial PD sample (PD (ind)) was obtained from Mondi and used as received. Elemental analysis showed that the sample also contains a certain amount of ammonium (0.10 %) and sodium ions (0.49 %), most likely from NH_4Cl and NaCl.

Silicon wafers with a thickness of 675 ± 25 μm were purchased from Siegert Wafers Aachen (Germany). SPR sensor slides (CEN102Au) with a chromium adhesion layer on glass and a gold coating (approx. 50 nm) were obtained from Cenibra (Bramsche, Germany). QCM-D crystals (QSX 301 Gold) coated with an Au-layer (approximately 100 nm) by aid of a chromium adhesion layer were purchased from Quantum Design Europe (Darmstadt, Germany).

2.2. Substrate cleaning and film preparation

The Au–glass sensors slides for surface plasmon resonance spectroscopy (SPR) measurements need to be cleaned prior use in order to remove all potential adventitious carbon from the surface. This cleaning is conducted by placing the sensor slides in a piranha solution which is prepared from sulfuric acid and hydrogen peroxide (30 wt%) in a 3:1 (v/v) ratio for max 6 min. Subsequent, the sensor slides were extensively rinsed with MQ water and dried in a stream of nitrogen. QCM-D Au-crystals were immersed into a mixture of H_2O/H_2O_2 (30 wt%) /NH_4OH (5:1:1; v/v/v) for 15 min at 70 °C, then treated with piranha solution containing H_2SO_4 / H_2O_2 (30 wt%) (3:1; v/v) for 60 s and afterwards extensively rinsed with MQ water and finally dried in a stream of nitrogen.

After cleaning of the sensor slides thin films from cellulose were prepared applying the spin coating technique. For SPR and QCM-D experiments cellulose thin films from two different cellulose precursors were prepared by use of (a) a 0.75 wt% trimethylsilyl cellulose (TMSC) solution in chloroform and (b) a 1.3 wt% cellulose xanthate (CX) aqueous solution. For film coating, 80 μl of cellulose derivative solution (per square centimeter of substrate) were deposited on the sensor slide which is then rotated for 60 s at a spinning speed of 4000 rpm and an acceleration of 2500 rpm·s^{-1} Afterwards the thin films were placed in a petri dish (5 cm diameter) and either 3 ml diluted HCl (10 %) for TMSC films or concentrated HCl (37 %) for CX based films were deposited next to the films. After covering the dish with its lid, the films were exposed for 15 min (TMSC thin films) and 25 min (CX thin films) to the HCl vapors. The CX based thin films required a washing step prior further use in order to remove NaCl crystals which have formed during regeneration. Therefore, the films were rinsed with 3 ml MQ water (3 times) and afterwards dried in a stream of nitrogen [44]. The cellulose films from TMSC were ready to use after regeneration. ATR-IR spectroscopy was used to verify that the regeneration to cellulose was complete as reported in literature [45,46].

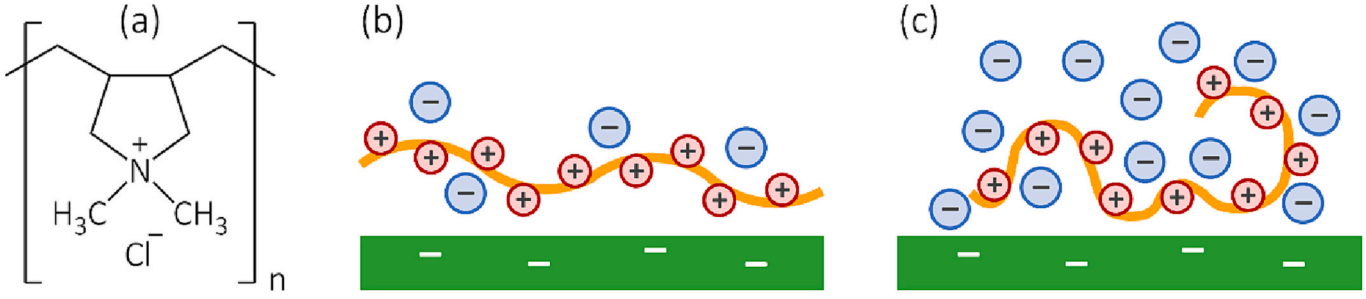

Fig. 1. (a) Molecular structure of PD. (b) Schematic representation of the conformation of the cationic polyelectrolyte adsorbed on a slightly anionic cellulose surface (green) from an aqueous solution without added electrolyte and (c) in presence of added electrolyte. (For interpretation of the references to color in this figure legend, the reader is referred to the web version of this article.)

2.3. Infrared spectroscopy – ATR-IR

Infrared spectra were recorded with an Alpha FT-IR spectrometer (Bruker, Billerica, MA, USA) applying an attenuated total reflection (ATR) attachment. The spectra were attained with 64 scans and a resolution of 4 cm^{-1} in a scan range between 400 and 4000 cm^{-1}. For ATR-IR measurements the sample thin films were prepared on gold coated glass slides. For data analysis, the OPUS 4.0 software was used.

2.4. Refractometry

The Abbemat 550 Performance Refractometer from Anton Paar (Graz, Austria) was applied for refractive index (RI) measurements. The measurements were conducted at T = 25 °C using a 589 nm laser.

2.5. Density meter

The DMA 4500 M Density Meter from Anton Paar (Graz, Austria) was utilized to determine the density of different liquids. For the measurements a U-tube from borosilicate glass is applied at T = 25 ± 0.02 °C for a measurement period of ca. 1 min using approximately 1 ml of sample solution.

2.6. Profilometry

Profilometry measurements were performed to determine the cellulose layer thickness using a DETAK 150 Stylus Profiler from Veeco. The scan length was set to 1000 μm for a measurement period of 3 s. A diamond stylus with a radius of 12.5 μm was used. The measurements were conducted with a stylus force of 3 mg at a resolution of 0.333 μm sample and a measurement range of 6.5 μm. The coated films were scratched to remove parts of the cellulose thin film to measure the film thickness of the coating using a step-height profile. From the resulting profile the thickness of the films was calculated. The measurements were performed at least at six independent positions, for all samples prior and after regeneration.

2.7. Dynamic light scattering (DLS) and zeta-potential measurements

The PD samples were diluted with 8 mM and 170 mM NaCl-MQ solution (pH 7.5), respectively, to obtain a final sample concentration of 1 wt%. All experiments were performed at least in triplicate. To determine the hydrodynamic radius and the zeta-potential of the different PD samples the Litesizer™ 500 from Anton Paar (Graz, Austria) with a λ = 658 nm single-frequency laser diode (40 mW) was used. The measurements were performed at T = 25 °C using a sample volume of approximately 1 ml, performing 60 scans after an equilibration step of at least 5 min. The Anton Paar 'Kalliope™' software was used for the measurements and the evaluation of the data. To calculate the mean hydrodynamic radius the cumulant model ISO 22,412 was used. The analysis of the zeta-potential was conducted applying the Smoluchowski approximation with a Debye factor of 1.50.

2.8. Atomic force microscopy – AFM

Atomic Force Microscopy images were recorded in tapping mode in an ambient atmosphere and at room temperature using a Tosca™ 400 atomic force microscope from Anton Paar (Graz, Austria). Silicon cantilevers (AP-ARROW-NCR from NanoWorld AG, Neuchatel, Switzerland) having a resonance frequency of 285 kHz and a force constant of 42 $N{\cdot}m^{-1}$ were utilized. AFM image processing and root mean square roughness (RMS) calculation was completed with Tosca Analysis software (Anton Paar, Graz, Austria) and Gwyddion 2.53 software.

2.9. Multi parameter surface plasmon resonance spectroscopy – MP-SPR

MP-SPR spectroscopy measurements were performed operating a MP-SPR Navi210 VASA from BioNavis Ltd. (Tampere, Finland) having two measurement chambers equipped with lasers of different wavelengths (670, 785, 850, 980 nm). The measurements were carried out at T = 25 °C using a full angular scan from 39 to 78° at a scan speed of $8°{\cdot}s^{-1}$ using gold coated sensor slides. A general procedure for conducting the measurements was as follows. The cellulose thin films which have been spin coated onto the SPR sensor slides were equilibrated in MQ water or electrolyte solution (8, 170 mM NaCl) at a flow rate of 25 $\mu l{\cdot}min^{-1}$ for a period of at least 30 min. Afterwards, the PD sample solutions was introduced into the flow cell at a concentration of 1 %, and rinsed over the cellulose surface at a flow rate of 25 $\mu l{\cdot}min^{-1}$ over a period of 10 min. The concentration of 1 % is quite representative for cationization processes e.g. of regenerate fibers, however it has to be mentioned that PD concentrations in industrial applications like papermaking are up to 100 times lower. After successful adsorption of PD samples, the biopolymer films were again rinsed with the corresponding equilibration solution until a stable signal was detected. All experiments were performed at least in three parallels.

BioNavis Dataviewer software was used for data processing. De Feijter equation, Eq. (1), was used to calculate the amount of adsorbed PD Γ [$mg{\cdot}m^{-2}$] by using the change of the SPR angle $\Delta\Theta$ [°] during adsorption [47]. The term $k \times d_p$ [cm/°] can be considered constant for thin films (<100 nm) and can be calculated by calibrating the instrument by determining the decay wavelength l_d. For the MP-SPR Navi™ 210A VASA used in this study, the $k \cdot d_p$ values are 1.90×10^{-7} cm/° for the 785 nm laser in aqueous systems. The dn/dc values of the different PD samples were determined by refractometry at a wavelength of 589 nm at 20 °C (Abbemat 550, Anton Paar, Austria).

$$\Gamma = \frac{\Delta\Theta{\cdot}k{\cdot}d_p}{\frac{dn}{dc}} \tag{1}$$

Detection limit of the method is 0.1 $mg{\cdot}m^{-2}$. The refractive index increment dn/dc [$cm^3{\cdot}ml^{-1}$] of PD samples were determined by performing refractive index measurements of calibration solutions of different PD concentrations in equilibration solution at pH 7.5 and T = 25 °C, and different ionic strengths.

2.10. Quartz crystal microbalance with dissipation — QCM-D

A QCM-D from Q-Sense (Gothenburg, Sweden) with simultaneous detection of the resonance frequency f and energy dissipation of an oscillating piezoelectric crystal was employed. Dissipation describes the frictional losses which cause a damping of the oscillation in correlation to the viscoelastic properties to the materials absorbed on the crystals. Rigid layers are assumed to fully couple to the oscillation of the crystal, where the change in layer mass Δm as a function of frequency change Δf [Hz] is given by the Sauerbrey Eq. (2)

$$\Delta m = C\frac{\Delta f_n}{n}. \tag{2}$$

C is the Sauerbrey constant (−17.7 ng Hz^{-1} cm^{-2} for a 5 MHz crystal), Δm [ng] is the changing mass of the crystal due to the adsorbed layer and n is the dimensionless overtone number [48]. The swelling of the cellulose causes dissipation, leading to a measurement sensitivity of 0.3 $mg{\cdot}m^{-2}$. The baseline resonance frequencies for the crystals were determined before depositing the cellulose layers and subsequent determination of the water content in the layers was done with a H_2O/D_2O exchange experiment, as described by Kittle et al. [49,50].

By exploiting differences in viscosity and density between H_2O and D_2O, the amount of water uptake by the accessible parts of the thin films can be determined. Based on the Kanazawa [51] Eq. (3) we find:

$$\frac{\Delta f_{H2O}}{n} = \frac{\frac{\Delta f_{film}}{n} - \frac{\Delta f_{bare}}{n}}{\frac{\rho_{D2O}}{\rho_{H2O}} - 1} \quad (3)$$

where Δf_{film} and Δf_{bare} describe the frequency shifts caused by an exchange of H_2O by D_2O on a bare substrate and on substrates coated with the cellulose films respectively. The density ρ is 0.9982 g·cm^{-3} for pure H_2O, 0.99739 g·cm^{-3} for 8 mM NaCl in H_2O, 1.00419 g·cm^{-3} for 170 mM NaCl in H_2O, 1.1050 g·cm^{-3} for pure D_2O, 1.10493 g·cm^{-3} for 8 mM NaCl in D_2O, and 1.11161 g·cm^{-3} for 170 mM NaCl in D_2O solution at T = 25°, n is the dimensionless overtone number and Δf_{H2O} [Hz] is the frequency shift, induced by the water absorbed in the cellulose films. With the Sauerbrey Eq. (2), Δf_{H2O} can directly be transferred in a total water content Γ_{water} [mg·m^{-2}].

$$\Gamma_{water} = C^* \frac{\Delta f_{H2O}}{n} \quad (4)$$

After recording the resonance frequencies before and after coating, the QCM-D flow cell was flushed with MilliQ water (0.1 ml·min^{-1}) for 30 min. After equilibration, the water was exchanged with D_2O and the cells were flushed for another 30 min with D_2O. Finally, the system was changed back to water again. The H_2O/D_2O exchange was also done with uncoated crystals, as reference. The same procedure was also performed with H_2O and D_2O containing 8 and 170 mM NaCl. For each experiment, at least three parallel measurements have been performed. The determined mass of the exchanged water was then correlated to the film mass to adjust the results to the thickness of the films.

2.11. Data analysis

The measurement error for the result data has been calculated as the 95 % confidence limits of the mean. Before calculation of the mean value outliers have been removed from the data using the Dixon-Grubbs outlier test, also on 95 % confidence limit.

3. Results and discussion

3.1. Thin film preparation and characterization

To investigate the effects of differently charged cellulose surfaces on the adsorption/interaction potential with PD samples, we chose two different types of cellulose derivatives for film preparation, namely trimethylsilyl cellulose (TMSC) and cellulose xanthate (CX). These cellulose derivatives were manufactured into model thin films using the spin coating technique and the conversion to regenerated cellulose was accomplished by exposure to HCl vapor which cleaves the trimethylsilyl and xanthate groups according to established literature protocols. [44,46] To verify the regeneration, ATR—IR spectra of the regenerated cellulose thin films were recorded, showing a broad OH-band between 3200 and 3600 cm^{-1}. IR-bands originating from the precursors (e.g., ν_{SiC}, δ_{SiOC} at 1250 and 852 cm^{-1} for TMSC and $\nu_{C=S}$ at 1520 and 1050–1250 cm^{-1} for CX) were no longer observed after regeneration and rinsing with water. Regeneration of TMSC and CX thin films leads to a shrinkage in film thickness in z-direction by up to 50 % to give thin films with a thickness of 35 ± 3 nm for $TMSC_{reg}$ and 38 ± 2 nm for CX_{reg} films. The AFM images revealed that the films featured a root mean square (RMS) roughness of 1.3 nm for $TMSC_{reg}$ and 5.9 nm for CX_{reg} films. The higher surface roughness of the CX_{reg} films in comparison to the $TMSC_{reg}$ films originates from the hole-like surface features (see Fig. 2) caused by the formation of sodium chloride during regeneration on the surface, altering the morphology before they are finally washed off.

In previous studies, we identified differences in adsorption behavior of the two regenerated cellulose film systems and pointed out the importance of the cellulose substrate on the adsorption behavior.[52] An example is that the two regenerated cellulose surfaces feature different contributions to their surface free energy (SFE). $TMSC_{reg}$ films exhibit a lower polar SFE contribution (19 ± 2 mJ·m^{-2}) than regenerated thin films from cellulose xanthate (29 ± 2 mJ·m^{-2}). Further, a slightly higher negative zeta potential was recorded for CX_{reg} films (−29

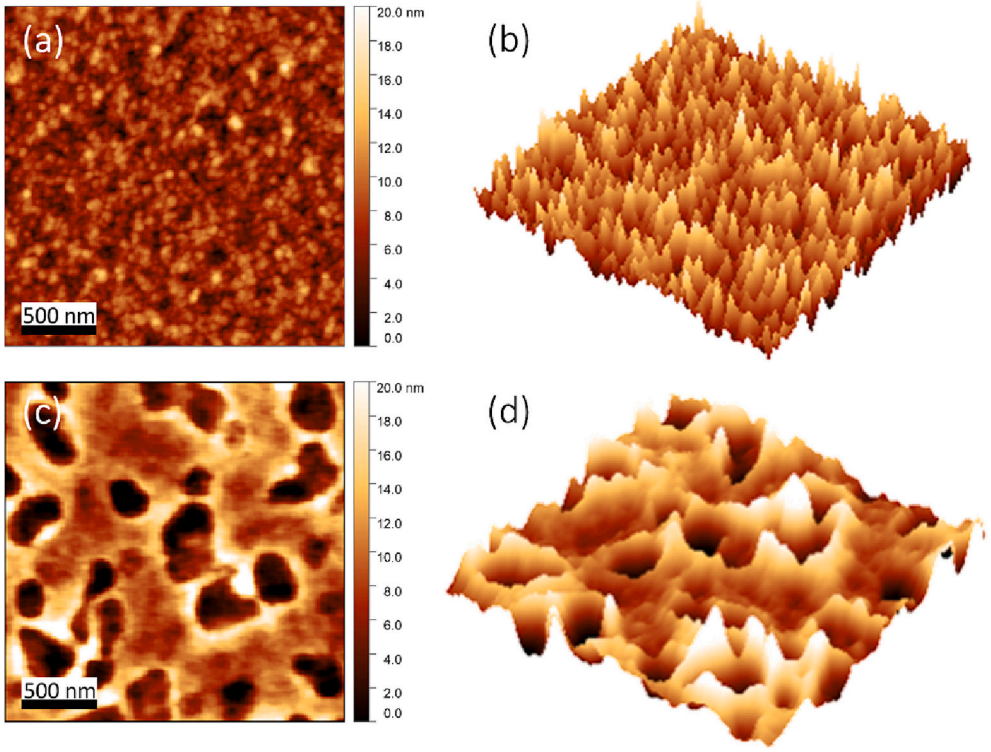

Fig. 2. Representative 2 × 2 μm^2 AFM topography images of (a) regenerated TMSC and (b) the corresponding 3-D surface image of $TMSC_{reg}$. In comparison the (c) topography image and (d) 3-D surface image of a regenerated CX film.

± 3 mV) than for the $TMSC_{reg}$ films (−23 ± 5 mV) at pH 6.5 in a 1 mM NaCl solution, which is an indication for the presence of a higher number of negative charges on the CX_{reg} films.

3.2. Characterization of PD in solution — particle size, zeta-potential and refractive index increments

For the adsorption studies on the thin films, PDs with low, medium and high molecular weight (PD_{low}, PD_{med} and PD_{high}) were used as well as a commercial product which is employed in industry (PD_{ind}). Accordingly, the properties of the PD compounds in solution were examined, i.e. the particle size (DLS), the zeta potential and the respective *dn/dc* values (needed for quantification of SPR data), were determined (see Table S1 in the SI).

DLS studies revealed that there are hardly any differences in size for all the samples. The size distributions are bimodally centered at ca 6–10 nm and between 100 and 900 nm (Fig. 3a). When looking at the number weighted distributions, the data clearly shows that there are only a few large particles present and the majority consists of a fraction below 10 nm (Fig. S1). The DLS correlation functions reveal an ideal exponential decay for PD_{med}, PD_{high} and PD_{ind}, which further supports these results. However, for PD_{low} a small feature in the exponential decay section of the correlation function was observed, indicating that also some larger particles (aggregates) may be present.

The zeta potentials of the PD samples increased with increasing molar mass and particle size (see Table S1), ranging from +22 mV (PD low) to nearly +30 mV (PD high), which is in agreement with other systems where higher absolute zeta potentials have been observed with increasing particle sizes [53]. The pH value did not impact the zeta potential neither at a concentration of 1 wt% nor at lower concentrations (0.01 %). The refractive index increments of most samples are similar at a given ionic strength and only show small deviations, with PD_{ind} being an exception, exhibiting much higher *dn/dc* values than the other samples.

3.3. Water content determination of regenerated cellulose thin films by QCM-D

Besides the differences in surface roughness and charge density of the cellulose surfaces, dissimilarities in the swelling behavior of the two regenerated cellulose systems may impact the interaction with adsorbing species. To investigate the water uptake and swelling behavior of regenerated cellulose thin films, H_2O-D_2O exchange experiments using QCM-D were performed. The results of these studies are depicted in Fig. 4.

For the bare gold crystal, a Δf_3 of ca. -64.2 Hz was determined for the H_2O and D_2O exchange, −65.9 Hz for solutions containing 8 mM NaCl and −66.0 Hz for those containing 170 mM NaCl (dashed grey lines).

For the $TMSC_{reg}$ films, the H_2O-D_2O exchange results in a Δf_3 of −79.3 ± 2.3 Hz (Fig. 4a). In the case of the 8 mM NaCl solution, the change is in a similar range with Δf_3 = 80.8 ± 1.9 Hz (Fig. 4b), while a slightly smaller change of about −78.4 ± 1.7 Hz was measured for the 170 mM NaCl solutions (Fig. 4c). The CX_{reg} thin films had larger total Δf_3 frequency shifts (ca. -96.6 ± 4.3 Hz for H_2O-D_2O, ca. -97.9 ± 3.9 Hz in 8 mM NaCl and ca. -96.1 ± 4.1 Hz in 170 mM NaCl). According to the frequency shifts the total amount of water was calculated and related to their respective dry masses. The $TMSC_{reg}$ films feature a water uptake capacity of 77 ± 3 %, which slightly increased at 8 mM NaCl to 80 ± 3 %. At high ionic strength (170 mM), it decreased to 66 ± 3 %. An even higher water uptake was monitored for CX_{reg} films. In MQ water and 8 mM NaCl the water uptake is 103 ± 6 % and 103 ± 5 % respectively. Similar to the $TMSC_{reg}$ films, the water uptake was reduced in the 170 mM NaCl solution to 96 ± 6 %. The measurements show that the swelling ability of CX_{reg} films is higher than that of $TMSC_{reg}$ surfaces, regardless of whether electrolytes are present or not. This trend is consistent with studies by Mohan et al. and Weißl et al. who investigated the swelling behavior of regenerated TMSC and CX thin films in pure water and reported a higher water uptake for CX_{reg} films [42,50,54].

In general, the water uptake of cellulosic materials is governed by the hydration of the hydroxyl groups in cellulose when exposed to water. Typically, most cellulosic materials feature a certain concentration/load of charged groups due to, for example oxidation but also residual hemicelluloses. The degree of swelling is reported to be substantially proportional to the effective charge density of the material [55]. Due to this, the higher water uptake capability of the regenerated CX thin films indicates a higher concentration of charged groups within this film system than in $TMSC_{reg}$ ones. Kontturi et al. evaluated the effect of additionally introduced charges on the swelling behavior. For CMC-modified CNF films, an increase in film swelling was observed at higher change density [55].

3.4. Adsorption behavior studies of PD on regenerated cellulose thin films by MP-SPR and AFM

To investigate the adsorption behavior of PD on the biopolymer thin films, surface plasmon resonance spectroscopy was used. The interaction performance of PD was studied in dependency of the PD molecular weight, the presence of electrolytes and the ionic strength, the

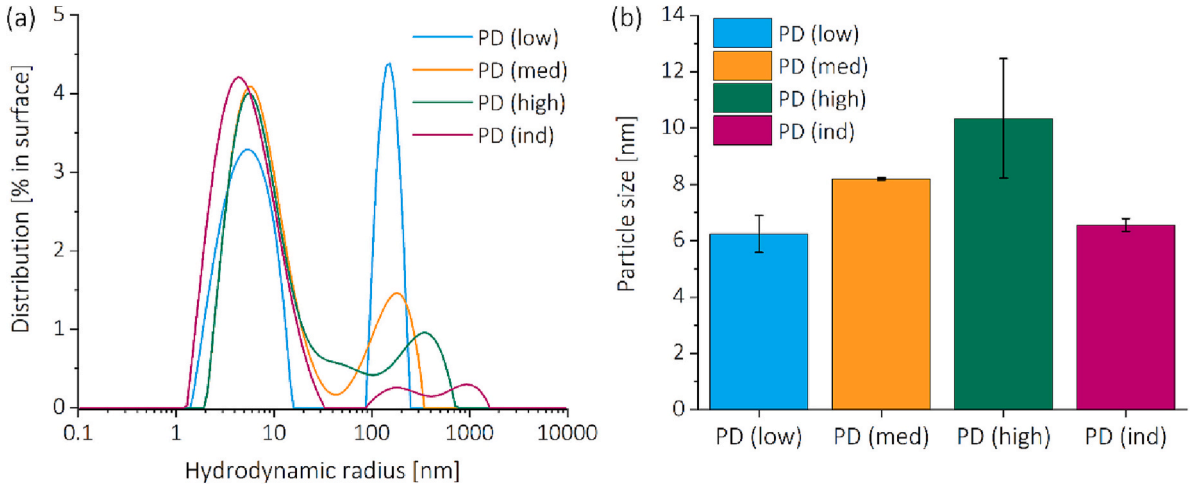

Fig. 3. Comparison of median hydrodynamic radii of the different PD compounds (c = 1 wt%) in aqueous solution (170 mM NaCl, pH 7.5) determined by DLS. (a) Intensity-weighted distribution of the full range. (b) Intensity-weighted size distribution of the area between 1 and 30 nm.

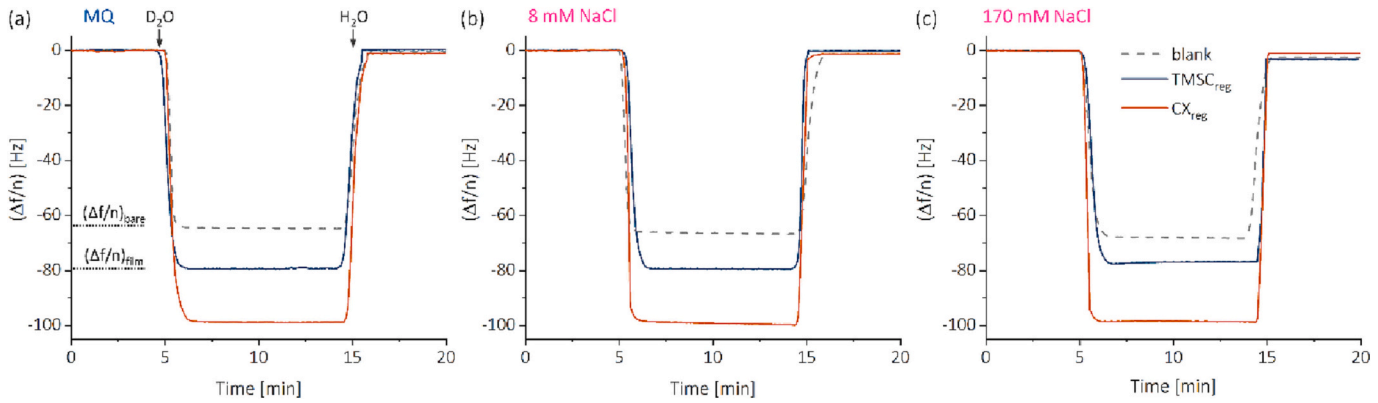

Fig. 4. H_2O-D_2O exchange experiments using Δf_3 to determine the water uptake capability of $TMSC_{reg}$ (blue line) and CX_{reg} (orange line) films. (a) pure H_2O-D_2O, (b) H_2O-D_2O containing 8 mM NaCl (c) H_2O-D_2O containing 170 mM NaCl. Flow rate: 0.1 ml·min^{-1}, T = 25 °C, pH 7.5. (For interpretation of the references to color in this figure legend, the reader is referred to the web version of this article.)

electrolyte species and the cellulose surface (morphology, charge and polarity).

The SPR sensogram curves of experiments performed in MQ water (Fig. 5a) and in 8 mM NaCl solution (Fig. 5b) at pH 7.5 on CX_{reg} thin films displayed fast adsorption for all PD compounds, as represented by the steep slope of the sensogram curves immediately after injection of the sample (at t = 10 min). In all experiments, the steady state, indicated by the formation of a plateau, was reached within the first minutes after sample injection for all PDs. The change in SPR angle during PD sample injection was in the range of 0.3° to 0.4° for all samples, but a clear trend in terms of molar mass of the PD samples was not observed. After 10 min, the surfaces were rinsed and equilibrated with MQ or 8 mM (start at t = 20 min). As soon as a stable signal was reached, the irreversibly adsorbed amounts of PD were determined by applying the De-Fejter Eq. (1).

There was only a weak trend that higher molar mass leads to an increase of PD surface concentration on CX_{reg} thin films (PD_{low}: 0.81 ± 0.15, PD_{med}: 0.91 ± 0.10 and PD_{high}: 1.07 ± 0.15 mg·m^{-2}, Fig. 5c). For the industrial compound, 0.80 ± 0.17 mg·m^{-2} of adsorbed PD on CX_{reg} thin films were determined. These values correspond to monolayer coverage on the cellulose surfaces. A similar monolayer type of adsorption for increasing molecular weight of cationic polymer on negatively charged surfaces has been observed in MQ water for polyacrylamide on silica [56]. By increase of electrolyte concentration to 8 mM NaCl, more coiling is expected, potentially leading to larger PD surface concentrations. However, for PD_{low} and PD_{med} only a slight increase of surface concentration was observed (0.91 ± 0.14 and 0.98 ± 0.13 mg·m^{-2}). The PD_{high} as well as the PD_{ind} exhibited much more pronounced irreversible adsorption onto the surfaces with 1.63 ± 0.23 and 1.92 ± 0.10 mg·m^{-2} respectively, corresponding to a doubling of adsorbed mass compared to experiments performed in MQ water.

The same experiments were further conducted on the $TMSC_{reg}$ thin films. A comparison of the adsorption data of the PD samples on both film systems shows Fig. 6. The adsorption of all PD compounds shows the same kinetics as for the CX_{reg} surfaces (fast formation of steady state, Fig. S2). However, the affinity of the PD samples to the surfaces is lower, indicated by a smaller change of SPR angle at the steady state conditions (0.15–0.25°) compared to the CX_{reg} thin films. Consequently, the surface concentrations of PD on the TMSC films after removing rinsing was lower with values in the range of 0.62 ± 0.09 to 0.67 ± 0.14 mg·m^{-2}. These values also did not increase by changing the adsorption conditions to 8 mM NaCl, and essentially the same results were obtained as in MQ water (0.62 ± 0.08 to 0.66 ± 0.05 mg·m^{-2}). An exception is PD_{ind} which doubled by adsorption from 8 mM NaCl (0.35 ± 0.16 mg·m^{-2}).

As the PD_{high} and the PD_{ind} samples showed the most interesting behavior, measurements using higher ionic strength (170 mM NaCl) were performed, also a change in pH (pH = 4) and electrolyte type ($CaCl_2$ at same ionic strengths) was investigated. At higher ionic strengths, the electrostatic interaction of the PDs with the cellulose surfaces is screened which is reflected in a massive decrease of the surface concentrations using such conditions on both surfaces. However, the decrease is more pronounced on the CX_{reg} surfaces than on the $TMSC_{reg}$ ones. At pH 7.5, slightly higher deposition of PDs was observed on the $TMSC_{reg}$ thin films (Fig. 7a). The decrease in pH value to 4 led to a lower adsorption of PD_{ind} on the films compared to pH 7 on both surfaces at all investigated conditions. A change of the electrolyte type (from NaCl to $CaCl_2$ at same ionic strength, Fig. 7c) revealed that Ca^{2+} ions are detrimental for PD adsorption, leading to lower PD surface concentrations on the CX_{reg} thin films. On $TMSC_{reg}$, films a slight increase was observed at 8 mM ionic strength, however, the surface concentration of PD_{ind} was still only half of the one on the CX_{reg} surfaces. The adsorption data is interpreted w.r.t. different aspects: influence of the PD species, effect of electrolyte and the role of the substrate.

3.4.1. *Differences between PDs and effect of ionic strength*

For the PD species, the solubility, the molar mass, the resulting zeta potential and the extent of coiling at certain electrolyte concentrations are the determining factors for adsorption. At low ionic strengths (e.g. MQ water), PEs in general adopt a flat conformation, resulting in the formation of monolayer type coverage. In general solubility of polymers decreases with increasing molar mass and if there is a specific interaction (e.g. electrostatics), the solubility at the interface is reduced, leading to enhanced adsorption in the case of the CX_{reg} films, while deposition remains constant on the $TMSC_{reg}$ films. The increase in ionic strength to 8 mM resulted in enhanced adsorption for the CX_{reg} thin films, which can be explained by coiling of the PD samples, thereby increasing the interaction capacity. The larger the molar mass, the more extended coiling will take place, resulting in lower solubility on negatively charged interfaces. These less charged substrates do not feature specific interactions and we speculate that adsorption of the PD samples on these films are driven by nonspecific adsorption mechanisms. An indication that this is the case stems from the results from adsorption experiments conducted at much higher ionic strengths (170 mM). Such high ionic strengths screen the surface charges and effectively prevent electrostatic interactions between PEs and an oppositely charged surface.

3.4.2. *Effect of electrolyte*

When changing the electrolyte type to $CaCl_2$ while maintaining the same ionic strength (8 mM NaCl corresponds to 2.7 mM $CaCl_2$, 170 mM NaCl corresponds to 57 mM $CaCl_2$, Fig. 7c), the adsorption tends to decrease. If a Ca^{2+} ion interacts with one OH group from the cellulose surface, a certain positive character of the divalent ion still remains. This further induces an electrostatic interaction with oppositely charged

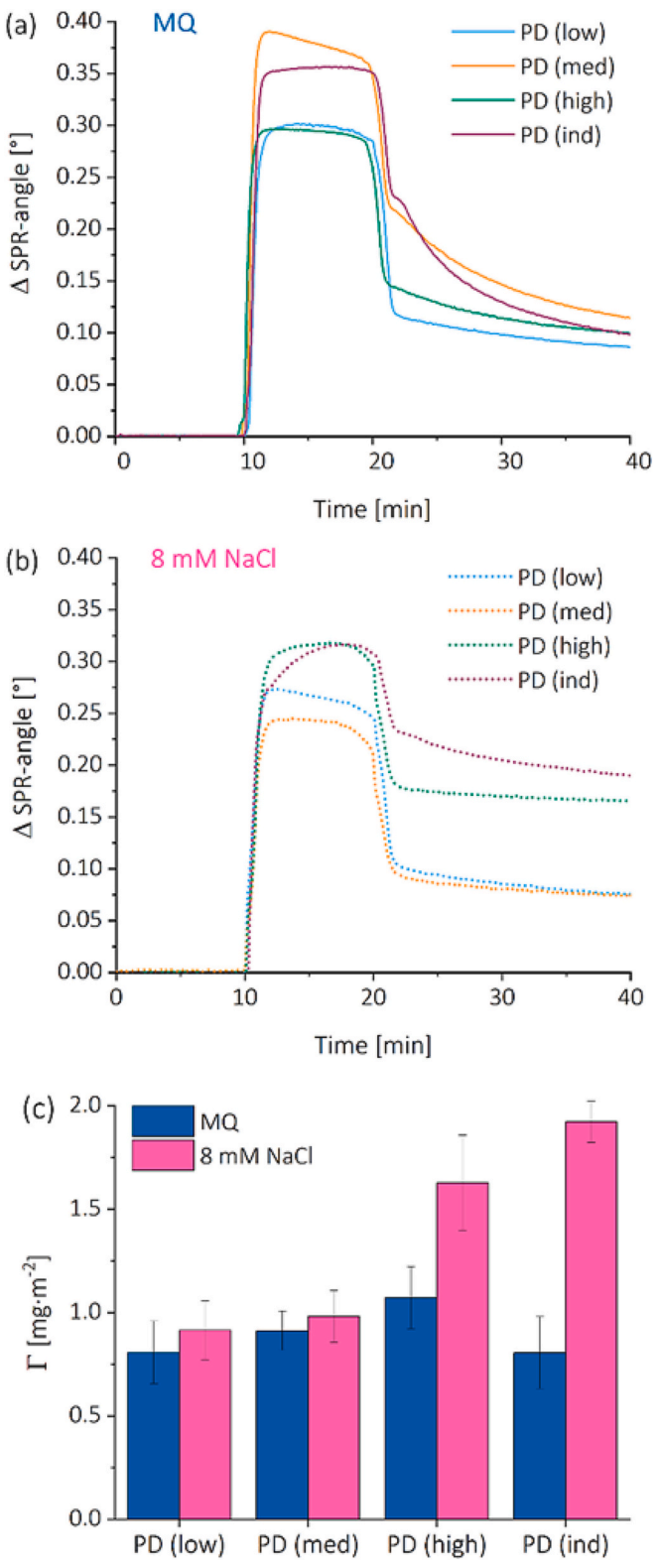

Fig. 5. PD adsorption (c = 1 wt%, at pH 7.5, 25 °C flow rate = 25 µl·min^{-1}) on CX_{reg} thin films from (a) MQ water and (b) 8 mM NaCl using SPR at λ = 785 nm and (c) corresponding irreversibly adsorbed surface concentration.

species, e.g. cellulose OH-groups or Cl^- ions within the reaction mixture. When Cl^- ions are attracted, it may be assumed that the interface short-range attractive forces which could attract cationic PD to the cellulose hydroxyl groups may become weaker resulting in less adsorbed PD molecules (shielding of the surface). This is in concurrence to attraction of PD to Cl^- ions in close vicinity to the surface. In short, the divalent ions may cause an accumulation of Cl^- ions close to the surface, what can cause a lowering in attraction forces between the cationic PD to the cellulose surface.

3.4.3. Differences between cellulose surfaces

Adsorption was consistently more pronounced in the case of the CX_{reg} films. These are more negatively charged than the $TMSC_{reg}$ films, and therefore the electrostatic interaction is larger with the PD samples. In addition, roughness is higher for the CX films, providing more available surface sites for adsorption. The molar mass of the PD samples does not seem to play a major role on the $TMSC_{reg}$ samples while at the CX_{reg} a slight increase was observed. At high ionic strength (170 mM) the adsorption of the PD samples on $TMSC_{reg}$ was much less reduced than for CX_{reg}. For the TMSC surfaces, we observed that the PD_{ind} exhibited nearly the same amount of adsorbed material at 8 and 170 mM NaCl at pH 7.5, also the PD_{high} sample adsorbed less at 170 mM but the absolute decrease was rather small (0.26 mg·m^{-2}) compared to 8 mM NaCl. In contrast, adsorption on the CX_{reg} thin films drastically reduced and was at that pH value even below that for the $TMSC_{reg}$ samples, further corroborating dominant electrostatic interactions in CX_{reg} films. At lower pH values, negatively charged groups (i.e. COOH) become (partially) protonated, thereby reducing the electrostatic interaction between surface and cationic polyelectrolyte further, which was indeed observed.

Changing the electrolyte from NaCl to $CaCl_2$, the adsorption tends to decrease the amount of deposited PD. This is consistent for the CX_{reg} surfaces, while for $TMSC_{reg}$ it is – considering error bars – remaining around the level for MQ water. At high ionic strengths, shielding becomes so dominant that the films behave similar, i.e. adsorption becomes really low.

Another point to consider is the surface morphology of the regenerated cellulose thin films. AFM topography images revealed a hole-like structure of the CX_{reg} surfaces with a higher surface roughness compared to the $TMSC_{reg}$ surfaces (see Fig. 2). The polyelectrolyte molecules are likely to adsorb uniformly on the surface, covering hills and filling cavities on a surface. Accordingly, the polycation can adjust its shape, which may lead to higher PD adsorption. AFM images acquired after adsorption of PD compounds from MQ and 8 mM NaCl (Figs. S3 and S4 in the SI) do not show major differences compared to the surfaces prior adsorption (Fig. 2). However, small roundish structures, probably PD agglomerates, can be seen in some images. After PD adsorption, a decrease in surface roughness is observed for all experiments, which supports the idea of surface roughness promoting PD adsorption.

The strength of the work presented lies in the analysis that PD adsorption can be very different for different cellulosic surfaces (CX_{reg} vs. $TMSC_{reg}$), and for quantifying the differences with complementary AFM and QCM-D measurements. However, there are still questions open, why the $TMSC_{reg}$ films' PD adsorption is showing a lower response to the PD molecular weight, electrolyte type or -concentration.

4. Conclusion

In this study, we investigated the impact of the molecular weight of PD compounds and the effect of electrolyte addition and concentration on the adsorption of the cationic PE with regard to differently charged cellulose substrates. The results should be regarded also in the context of regenerated fibers where cationization with polyelectrolytes is a common procedure. One of the applications is to improve the dyeing performance with anionic dyes, which can be promoted by addition of PD. Another relevant application is fiber adsorption and resulting performance of cationic additives in papermaking.

One result of our experiments is that the molecular weight of cationic PDs has only little to no effect on the amount of adsorbed PD on the cellulose surfaces in the absence of electrolytes. Increasing ionic strength (8 mM NaCl), the cationic PE molecules can dynamically

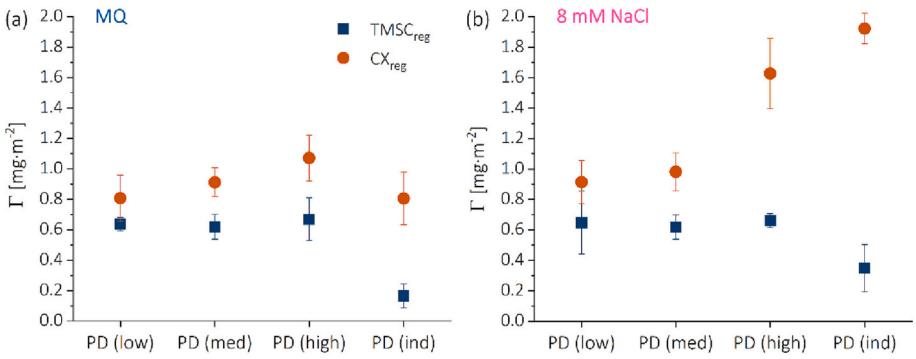

Fig. 6. Summary of results from adsorption experiments of PD (low), PD (med), PD (high) and PD (ind) on cellulose surfaces from $TMSC_{reg}$ (blue) and CX_{reg} (orange) applying SPR in (a) MQ and (b) 8 mM NaCl solutions at pH 7.5 and T = 25 °C. (For interpretation of the references to color in this figure legend, the reader is referred to the web version of this article.)

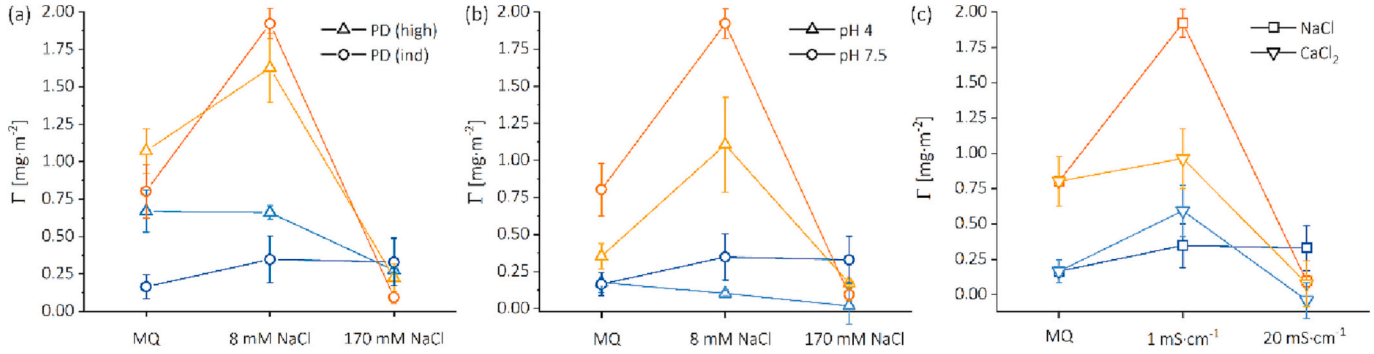

Fig. 7. Adsorption data of PD samples on the $TMSC_{reg}$ (blue) and CX_{reg} (orange) films using additional parameters (a) PD_{high} (triangles) and PD_{ind} (circles) at pH 7.5 (b) PD_{ind} at pH 4 (triangles) and pH 7.5 (circles) (c) PD_{ind} from NaCl (rectangle) and $CaCl_2$ (triangle) at pH 7.5. (For interpretation of the references to color in this figure legend, the reader is referred to the web version of this article.)

change their conformation from an elongated form to more coil-like structures [3]. Coiling, in combination with entropic effects trigger higher adsorbed amounts of the PD, most pronounced for high M_w and the industrial PD compound, the effect is strong for the CX_{reg} and quit weak $TMSC_{reg}$ surfaces. At high ionic strengths (170 mM) the cellulose surface charges are screened and PE interaction is impeded. At this high electrolyte concentration, the adsorbed amounts decreased significantly, and similar amounts of adsorbed PE were determined for all cellulose substrates and PD compounds.

Changing the electrolyte from NaCl to $CaCl_2$ while maintaining the same ionic strength, the adsorption tends to decrease. We speculate that the divalent ions may cause an accumulation of Cl^- ions close to the surface, lowering the attraction of the cationic PD to the cellulose surface.

The adsorption behavior was different for the CX_{reg} compared $TMSC_{reg}$ cellulose surfaces. It was in general much higher for the CX_{reg} films than for $TMSC_{reg}$. This can to some extent be attributed to a more negative zeta potential, a higher AFM roughness and a higher degree of swelling of the CX_{reg} substrates compared to the $TMSC_{reg}$ films. We furthermore speculate that for CX_{reg} the interaction is more by driven by electrostatics but for $TMSC_{reg}$ it seems to be of rather nonspecific nature. It can be concluded that differences in PD adsorption can be very different for different cellulose surfaces, and, apart from zeta potential, also differences in AFM nanoroughness and swelling of the cellulose films (as investigated with QCM-D) can contribute to explaining these differences.

CRediT authorship contribution statement

Carina Sampl: Conceptualization, Data curation, Formal analysis, Investigation, Methodology, Validation, Visualization, Writing – original draft. **Jana Schaubeder:** Data curation, Investigation. **Ulrich Hirn:** Conceptualization, Funding acquisition, Project administration, Writing – original draft, Writing – review & editing. **Stefan Spirk:** Conceptualization, Methodology, Supervision, Writing – original draft, Writing – review & editing.

Declaration of competing interest

The authors declare that they have no known competing financial interests or personal relationships that could have appeared to influence the work reported in this paper.

Acknowledgements

The financial support by the Austrian Federal Ministry for Digital and Economic Affairs and the National Foundation for Research Technology and Development is gratefully acknowledged. We also thank our industrial partners Mondi, Canon Production Printing, Kelheim Fibres, and SIG Combibloc for their financial support.

Appendix A. Supplementary data

Supplementary data to this article can be found online at https://doi.org/10.1016/j.ijbiomac.2023.124286.

References

[1] P.M. Claesson, E. Poptoshev, E. Blomberg, A. Dedinaite, Polyelectrolyte-mediated surface interactions, Adv. Colloid Interf. Sci. 114–115 (2005) 173–187.

[2] D. Scheepers, B. Chatillon, Z. Borneman, K. Nijmeijer, Influence of charge density and ionic strength on diallyldimethylammonium chloride (DADMAC)-based polyelectrolyte multilayer membrane formation, J. Membr. Sci. 617 (2021), 118619.
[3] A.V. Dobrynin, M. Rubinstein, Theory of polyelectrolytes in solutions and at surfaces, Prog. Polym. Sci. 30 (2005) 1049–1118.
[4] J. Kim, G. Kim, P.S. Cremer, Investigations of polyelectrolyte adsorption at the solid/liquid interface by sum frequency spectroscopy: evidence for long-range macromolecular alignment at highly charged quartz/water interfaces, J. Am. Chem. Soc. 124 (2002) 8751–8756.
[5] M. Ullner, C.E. Woodward, Orientational correlation function and persistence lengths of flexible polyelectrolytes, Macromolecules 35 (2002) 1437–1445.
[6] C. Chen, M. Ek, Antibacterial evaluation of CNF/PVAm multilayer modified cellulose fiber and cellulose model surface, Nord. Pulp Pap.Res. J. 33 (2018) 385–396.
[7] C. Chen, T. Petterson, J. Illergård, M. Ek, L. Wågberg, Influence of cellulose charge on bacteria adhesion and viability to PVAm/CNF/PVAm-modified cellulose model surfaces, Biomacromolecules 20 (2019) 2075–2083.
[8] L. Fras-Zemljič, V. Kokol, D. Čakara, Antimicrobial and antioxidant properties of chitosan-based viscose fibres enzymatically functionalized with flavonoids, Text. Res. J. 81 (2011) 1532–1540.
[9] L. Fras Zemljic, O. Sauperl, I. But, A. Zabret, M. Lusicky, Viscose material functionalized by chitosan as a potential treatment in gynecology, Text. Res. J. 81 (2011) 1183–1190.
[10] A.P. Gomes, J.F. Mano, J.A. Queiroz, I.C. Gouveia, Layer-by-layer deposition of antimicrobial polymers on cellulosic fibers: a new strategy to develop bioactive textiles, Polym. Adv. Technol. 24 (2013) 1005–1010.
[11] J. Illergård, U. Römling, L. Wågberg, M. Ek, Biointeractive antibacterial fibres using polyelectrolyte multilayer modification, Cellulose 19 (2012) 1731–1741.
[12] J. Illergård, L. Wågberg, M. Ek, Contact-active antibacterial multilayers on fibres: a step towards understanding the antibacterial mechanism by increasing the fibre charge, Cellulose 22 (2015) 2023–2034.
[13] Z. Li, X. Liu, X. Zhuang, Y. Guan, K. Yao, Manufacture and properties of chitosan/N, O-carboxymethylated chitosan/viscose rayon antibacterial fibers, J. Appl. Polym. Sci. 84 (2002) 2049–2059.
[14] N. Bairagi, M.L. Gulrajani, B.L. Deopura, A. Shrivastava, Dyeing of N-modified viscose rayon fibres with reactive dyes, Color. Technol. 121 (2005) 113–120.
[15] J. Koh, I. Soo Kim, S. Soo Kim, W. Sub Shim, J. Pil Kim, S. Yeop Kwak, S. Wook Chun, Y. Ku Kwon, Dyeing properties of novel regenerated cellulosic fibers, J. Appl. Polym. Sci. 91 (2004) 3481–3488.
[16] S. Sombatdee, S. Saikrasun, Structures and dyeing performances of polyethyleneimine-carbamate linked bamboo viscose fibers dyed with lac, Text. Res. J. 90 (2019) 179–193.
[17] H. Zeng, R.-C. Tang, Adsorption properties of direct dyes on viscose/chitin bicomponent fiber: evaluation and comparison with viscose fiber, RSC Adv. 4 (2014) 38064–38072.
[18] N. Aarne, E. Kontturi, J. Laine, Carboxymethyl cellulose on a fiber substrate: the interactions with cationic polyelectrolytes, Cellulose 19 (2012) 2217–2231.
[19] L.-E. Enarsson, L. Wågberg, Polyelectrolyte adsorption on thin cellulose films studied with reflectometry and quartz crystal microgravimetry with dissipation, Biomacromolecules 10 (2009) 134–141.
[20] M. Eriksson, A. Torgnysdotter, L. Wågberg, Surface modification of wood fibers using the polyelectrolyte multilayer technique: effects on fiber joint and paper strength properties, Ind. Eng. Chem. Res. 45 (2006) 5279–5286.
[21] A.E. Horvath, T. Lindström, J. Laine, On the indirect polyelectrolyte titration of cellulosic fibers. Conditions for charge stoichiometry and comparison with ESCA, Langmuir 22 (2006) 824–830.
[22] A.T. Horvath, A.E. Horvath, T. Lindström, L. Wågberg, Diffusion of cationic polyelectrolytes into cellulosic fibers, Langmuir 24 (2008) 10797–10806.
[23] D. Hu, T. Zhang, S. Zhang, J. He, X. Dong, Diffusion of polyethyleneimine with different molecular weights into cotton fibers at low concentration, Cellulose 28 (2021) 3997–4008.
[24] S. Strnad, O. Sauperl, L. Fras-Zemljic, Cellulose fibers functionalized by chitosan: characterization and application, in: M. Elnashar (Ed.), Biopolymers, IntechOpen, 2010, pp. 181–985.
[25] H. Zhang, C. Zhao, Z. Li, J. Li, The fiber charge measurement depending on the poly-DADMAC accessibility to cellulose fibers, Cellulose 23 (2016) 163–173.
[26] L. Fras Zemljič, Z. Peršin, P. Stenius, Improvement of chitosan adsorption onto cellulosic fabrics by plasma treatment, Biomacromolecules 10 (2009) 1181–1187.
[27] M. Korica, Z. Peršin, S. Trifunović, K. Mihajlovski, T. Nikolić, S. Maletić, L. Fras Zemljič, M.M. Kostić, Influence of different pretreatments on the antibacterial properties of chitosan functionalized viscose fabric: TEMPO oxidation and coating with TEMPO oxidized cellulose nanofibrils, Materials 12 (2019) 3144.
[28] C. Payerl, M. Bracic, A. Zankel, W.J. Fischer, M. Kaschowitz, E. Froehlich, R. Kargl, F. Stelzer, S. Spirk, Nonspecific protein adsorption on cationically modified Lyocell fibers monitored by zeta potential measurements, Carbohydr. Polym. 164 (2017) 49–56.
[29] T. Genco, L.F. Zemljič, M. Bračič, K. Stana-Kleinschek, T. Heinze, Characterization of viscose fibers modified with 6-deoxy-6-amino cellulose sulfate, Cellulose 19 (2012) 2057–2067.
[30] T. Köhnke, C. Pujolras, J.P. Roubroeks, P. Gatenholm, The effect of barley husk arabinoxylan adsorption on the properties of cellulose fibres, Cellulose 15 (2008) 537.
[31] A. Miletzky, M. Punz, A. Zankel, S. Schlader, C. Czibula, C. Ganser, C. Teichert, S. Spirk, S. Zoehrer, W. Bauer, R. Schennach, Modifying cellulose fibers by adsorption/precipitation of xylan, Cellulose 22 (2015) 189–201. Dordrecht, Neth.
[32] G. Findenig, R. Kargl, K. Stana-Kleinschek, V. Ribitsch, Interaction and structure in polyelectrolyte/clay multilayers: a QCM-D study, Langmuir 29 (2013) 8544–8553.
[33] K.S. Kontturi, T. Tammelin, L.-S. Johansson, P. Stenius, Adsorption of cationic starch on cellulose studied by QCM-D, Langmuir 24 (2008) 4743–4749.
[34] T. Mohan, T. Ristic, R. Kargl, A. Doliska, S. Koestler, V. Ribitsch, J. Marn, S. Spirk, K. Stana-Kleinschek, Cationically rendered biopolymer surfaces for high protein affinity support matrices, Chem. Commun. 49 (2013) 11530–11532. Cambridge, U. K.
[35] K. Niegelhell, A. Chemelli, J. Hobisch, T. Griesser, H. Reiter, U. Hirn, S. Spirk, Interaction of industrially relevant cationic starches with cellulose, Carbohydr. Polym. 179 (2018) 290–296.
[36] A.L. Da Róz, F.L. Leite, L.V. Pereiro, P.A.P. Nascente, V. Zucolotto, O.N. Oliveira, A. J.F. Carvalho, Adsorption of chitosan on spin-coated cellulose films, Carbohydr. Polym. 80 (2010) 65–70.
[37] L.-E. Enarsson, L. Wågberg, J. Carlén, N. Ottosson, Tailoring the chemistry of polyelectrolytes to control their adsorption on cellulosic surfaces, Colloids Surf. A Physicochem. Eng. Asp. 340 (2009) 135–142.
[38] J. Salmi, M. Österberg, P. Stenius, J. Laine, Surface forces between cellulose surfaces in cationic polyelectrolyte solutions: the effect of polymer molecular weight and charge density, Nord. PulpPap.Res.J. 22 (2007) 249–257.
[39] J. Su, C.J. Garvey, S. Holt, R.F. Tabor, B. Winther-Jensen, W. Batchelor, G. Garnier, Adsorption of cationic polyacrylamide at the cellulose–liquid interface: a neutron reflectometry study, J. Colloid Interface Sci. 448 (2015) 88–99.
[40] S.M. Notley, Effect of introduced charge in cellulose gels on surface interactions and the adsorption of highly charged cationic polyelectrolytes, Phys. Chem. Chem. Phys. 10 (2008) 1819–1825.
[41] T. Saarinen, M. Österberg, J. Laine, Adsorption of polyelectrolyte multilayers and complexes on silica and cellulose surfaces studied by QCM-D, Colloids Surf. A Physicochem. Eng. Asp. 330 (2008) 134–142.
[42] T. Tammelin, T. Saarinen, M. Österberg, J. Laine, Preparation of Langmuir/Blodgett-cellulose surfaces by using horizontal dipping procedure. Application for polyelectrolyte adsorption studies performed with QCM-D, Cellulose 13 (2006) 519.
[43] R. Alen, Papermaking Science And Technology: Papermaking Chemistry, Finnish Paper Engineers' Association, Helsinki, Finland, 2007.
[44] M. Weissl, K. Niegelhell, D. Reishofer, A. Zankel, J. Innerlohinger, S. Spirk, Homogeneous cellulose thin films by regeneration of cellulose xanthate: properties and characterization, Cellulose (2018) 711–721. Dordrecht, Neth.
[45] A.O.F. Jones, R. Resel, B. Schrode, E. Machado-Charry, C. Roethel, B. Kunert, I. Salzmann, E. Kontturi, D. Reishofer, S. Spirk, Structural order in cellulose thin films prepared from a trimethylsilyl precursor, Biomacromolecules 21 (2020) 653–659.
[46] E. Kontturi, S. Spirk, Ultrathin films of cellulose: a materials perspective, Front. Chem. 7 (2019) 488. Lausanne, Switz.
[47] J.A. De Feijter, J. Benjamins, F.A. Veer, Ellipsometry as a tool to study the adsorption behavior of synthetic and biopolymers at the air–water interface, Biopolymers 17 (1978) 1759–1772.
[48] G. Sauerbrey, Verwendung von Schwingquarzen zur Wägung dünner Schichten und zur Mikrowägung, Z. Phys. 155 (1959) 206–222.
[49] J.D. Kittle, X. Du, F. Jiang, C. Qian, T. Heinze, M. Roman, A.R. Esker, Equilibrium water contents of cellulose films determined via solvent exchange and quartz crystal microbalance with dissipation monitoring, Biomacromolecules 12 (2011) 2881–2887.
[50] T. Mohan, S. Spirk, R. Kargl, A. Doliska, A. Vesel, I. Salzmann, R. Resel, V. Ribitsch, K. Stana-Kleinschek, Exploring the rearrangement of amorphous cellulose model thin films upon heat treatment, Soft Matter 8 (2012) 9807–9815.
[51] K.K. Keiji, J.G. Gordon, The oscillation frequency of a quartz resonator in contact with liquid, Anal. Chim. Acta 175 (1985) 99–105.
[52] C. Sampl, S. Spirk, S. Eyley, W. Thielemans, U. Hirn, Real-time adsorption of optical brightening agents on cellulose thin films, Carbohydr. Polym. 261 (2021), 117826.
[53] E. Ofir, Y. Oren, A. Adin, Electroflocculation: the effect of zeta-potential on particle size, Desalination 204 (2007) 33–38.
[54] M. Weissl, M.A. Hobisch, L.S. Johansson, K. Hettrich, E. Kontturi, B. Volkert, S. Spirk, Cellulose carbamate derived cellulose thin films: preparation, characterization and blending with cellulose xanthate, Cellulose 26 (2019) 7399–7410. Dordrecht, Neth.
[55] K.S. Kontturi, E. Kontturi, J. Laine, Specific water uptake of thin films from nanofibrillar cellulose, J. Mater. Chem. A 1 (2013) 13655–13663.
[56] X. Zhang, Y. Zhu, X. Wang, P. Wang, J. Tian, W. Zhu, J. Song, H. Xiao, Revealing adsorption behaviors of amphoteric polyacrylamide on cellulose fibers and impact on dry strength of fiber networks, Polymers 11 (2019) 1886.